

**Picket Pulse Shaping with Phase and Amplitude  
Modulation in the Frequency Domain**

**Megan Alexander**

# Pulse Shaping with Phase and Amplitude Modulation in the Frequency Domain

Megan Alexander

Advisors: Wolf Seka and Jonathan Zuegel

## LABORATORY FOR LASER ENERGETICS

University of Rochester

250 East River Road

Rochester, NY, 14623-1299

### ABSTRACT:

The conversion of transform-limited short laser pulses to shaped longer pulses with frequency chirp was investigated. A program was created to simulate how transform-limited short input pulse shapes can be converted into output pulses of desired temporal shape and phase. The program models both electric field and spectral intensities of the pulses, conserves energy, and accounts for spectral limitations set by the input pulse and experimental system limitations. This work serves as foundation for further studies of pulse shaping using transform-limited mode-locked input pulse trains.

### INTRODUCTION:

Inertial confinement fusion (ICF) laser pulse shapes consist of a long “foot” forerunning the main pulse (Fig. 1). Replacing the low intensity foot pulse with a picket-fence pulse train has been suggested<sup>1</sup> to increase efficiency and power balance of ICF lasers. Therefore, investigating methods to provide arbitrary control of picket pulse shapes is deemed worthwhile.

Current pulse stretching methods employ diffraction gratings, which broaden the pulse, but do not allow arbitrary control of the resulting pulse phase. Pulse shaping through phase and amplitude modulation in the frequency domain would make the results more flexible and can be simulated computationally using such tools as MATLAB, the selected approach for this endeavor. MATLAB has many convenient tools to compute the pulse shape with and without phase chirp, as well as the corresponding spectra.

Specifications for laser pulses relate to ideal ICF conditions. Typical ICF implosion experiments require at least sixty large beams with identical well-defined pulse shapes. To achieve this, a very high degree of control of the laser pulse shapes and laser

amplification process is required. For laser physics reasons it turns out that picket-fence pulses may be preferable to continuous pulses. Hence the present pulse shaping code is a start to study picket-fence pulse shaping. Generally, a pulse with constant intensity can be well approximated by the average of a series of short, appropriately spaced, higher intensity pulses (see Fig. 1). The individual pulses of this series may have various pulse characteristics such a pulse shape or duration and/or time-varying frequency or phase (frequency chirp).

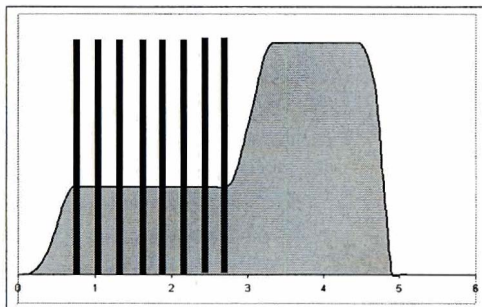


Figure 1: A standard ICF pulse with and without pickets.

The purpose of this project was to determine whether, to what degree, and how mode-locked laser pulses may be stretched through amplitude and phase changes in

the frequency domain. Keeping basic laws of physics in mind, like energy conservation, and allowing for various output pulse characteristics, a MATLAB program was developed to simulate this process. This program, FIREFLY simulates and compares input and output pulses under ideal conditions as well as non-optimal ones. The current version allows for single pulse generation only, though the same concepts apply to more complex scenarios involving pulse trains.

The desired output pulse is defined in the temporal domain both in terms of pulse shape and time-varying phase. For convenience we have chosen output pulses whose center frequencies change linearly during the pulse – also called a frequency chirp – that corresponds

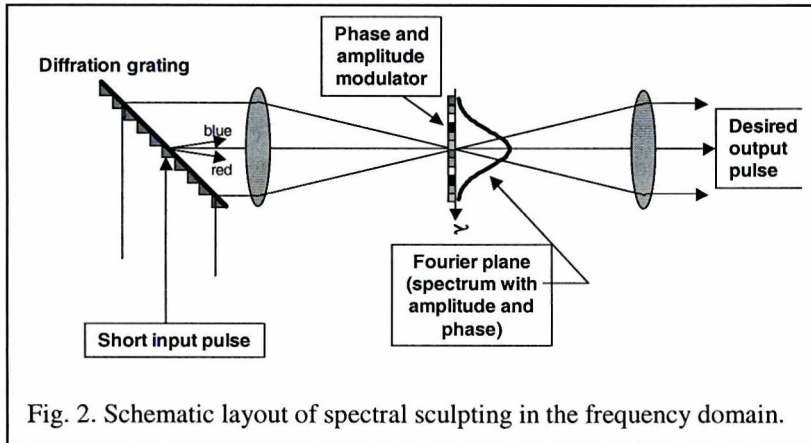


Fig. 2. Schematic layout of spectral sculping in the frequency domain.

to a quadratically changing phase with time. We then transform the input pulse and the desired output pulse mathematically into the spectral domain via Fourier transforms. Comparison of the input and desired output spectra in terms of amplitude *and* phase

then allows the specification of the Fourier amplitude and phase filters (or masks). It also allows the calculation of the efficiency of such devices. Thus, while the simulations impose the phase chirp in the temporal domain the real phase and amplitude modifications would be applied in the frequency domain.

Experimentally, one accesses the frequency domain by propagating the laser pulse through a diffraction grating followed by a converging lens. In the focal plane of this lens the pulse spectrum is dispersed as shown schematically in Fig. 2. This plane is the Fourier plane of the input pulse as well as the output pulse.

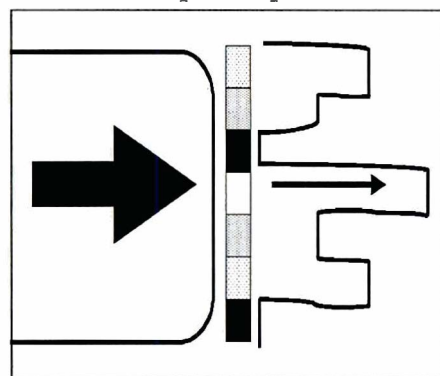


Figure 3: LCDs of varying transmission control the passage of an initially square beam (with frequencies dispersed in the vertical direction) through a sculping device. The output depends on the arrangement of LCDs.

Modifying the intensity or phase of different spectral components of the input laser pulse is then achieved by placing a mask (or masks, also called filters) in this plane as shown in Figures 2 and 3. These masks have spatially varying transmission or indices of refraction. The former changes the spectral pulse shape of the output pulse while the latter changes the optical path of a particular spectral component and thus its phase. These masks are typically linear arrays of liquid crystal devices (LCD) whose transmission or index of refraction depends on the applied voltage. Operating like miniature traffic signals, these cells may change the transmission for different lanes of light, thus sculping the spectrum of the beam (Fig. 3). To convert the output pulse back

into the temporal domain, it is passed through another lens (see Fig. 2).

It is of interest to note that the phase of a particular frequency component is really an angle whose magnitude is determined by the frequency chirp we desire for the

output pulse. While this angle may be computed to be very large, one may add or subtract any multiple of  $2\pi$  radians ( $360^\circ$ ) to this angle without affecting the (output) pulse shape. Thus the phase mask only needs to modify the phase of any particular spectral component within 0 and  $2\pi$ . The exact phase angle change is obtained by adding or subtracting an appropriate multiple of  $2\pi$  from the phase change computed by the Fourier transform of the desired output pulse. Thus a desired phase change of  $370^\circ$  is equivalent to a phase change of  $10^\circ$ .

Another consequence of the Fourier relationship between time domain and frequency domain can be seen in Fig. 4. A single short pulse has a broad continuous spectrum indicated with the “individual picket” heading. The spectrum of a series (or train) of the same pulses leads to a channeled spectrum with the same envelope as the single pulse spectrum (sidebands). Computationally, the Fourier transform between time domain and frequency domain is obtain using fast Fourier transform algorithms (FFT). A similar algorithm is used for the inverse process (IFFT) that allows transitioning from the frequency domain to the temporal domain.

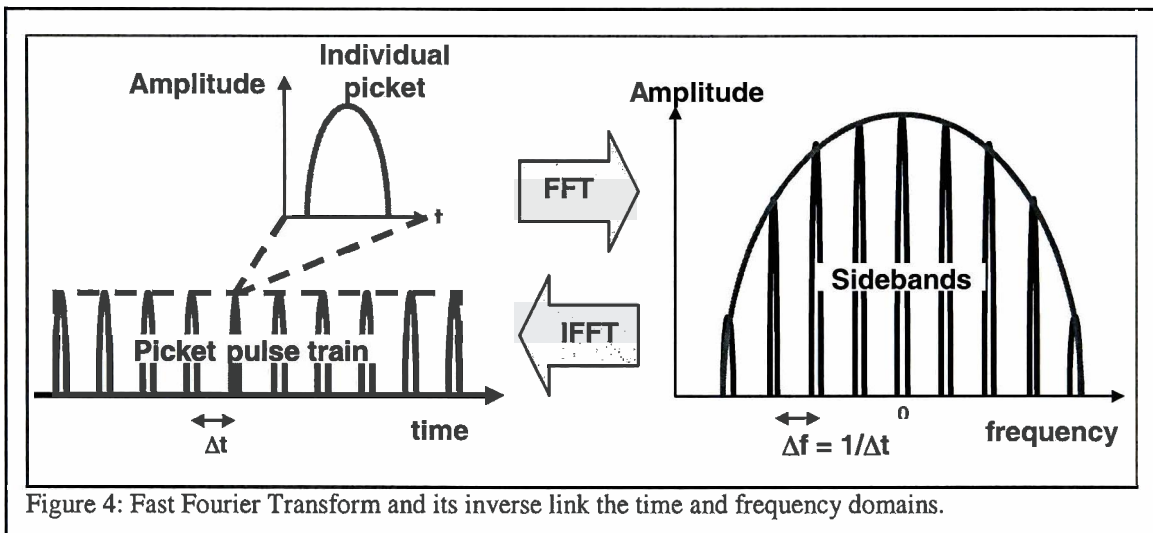


Figure 4: Fast Fourier Transform and its inverse link the time and frequency domains.

**METHODS:** FIREFLY simulates this experimental process by completing the same sequence of tasks: starting from an electric field for the short input pulse, its spectrum is obtained using a FFT conversion. Similarly, the desired output pulse is transformed to the spectral domain using a FFT conversion. Comparing the input and desired output spectra allows specification of the amplitude transmission and phase masks. In the present project we have restricted ourselves to comparing the input and output spectra in intensity and phase from which we also compute throughput efficiencies. The actual mask characteristics have not been computed explicitly but the spectral mask is obtained from simple ratios of the spectral intensities of the output and input pulses while the phase mask (within modulo  $2\pi$ ) is given by the calculated (desired) output phases (the input phase is constant and can be neglected since we have assumed a transform-limited input pulse shape).

The input to FIREFLY is a short (1-5 ps) laser pulse and its spectrum is calculated via fast Fourier transform simulating the effect of a grating and the lens in Fig. 2. We similarly calculate the spectrum for a specific requested output pulse (Full Width at Half Max [FWHM], pulse shape [Gaussian, super-Gaussian, sech], and phase [corresponding to a frequency chirp]).

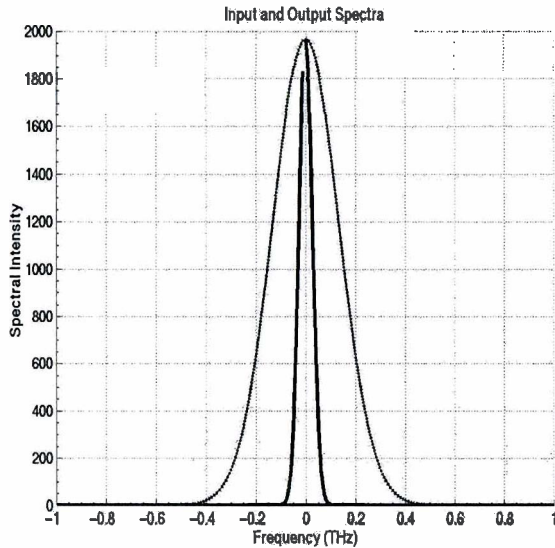


Figure 5: The spectrum of the wider output pulse fits entirely underneath that of the 2ps input pulse.

The short pulse has a corresponding broad spectrum (large bandwidth). The spectrum of the requested output pulse must fit under the envelope of the input pulse (Figure 5).

A transform-limited long output pulse has a much narrower spectrum than the input pulse as shown in Fig. 5. If the desired output pulse has an impressed frequency chirp the corresponding spectrum is wider and can more nearly (or completely) match the input spectrum. When the input and output spectra are identical, a maximum throughput efficiency of 100% can be achieved. Other conditions make sculpting much like the round peg and square hole paradox,

i.e., energy must be thrown away in order to return the desired pulse. This is expected and FIREFLY typically returns several alternatives along with the corresponding throughput efficiencies.

The area under the spectral intensity curves shown in Fig. 5 represents the pulse energy. Since the output spectral intensity must not exceed the input spectrum anywhere, the transform-limited long pulse contains much less energy than the short input pulse, leading to a low throughput efficiency. For desired output pulses with large frequency chirp and correspondingly large bandwidth (spectrum) we may have to take advantage of the extended spectral wings of the input pulse that are not easily visible in linear graphs such as Fig. 5. We must then force the output spectrum to fall

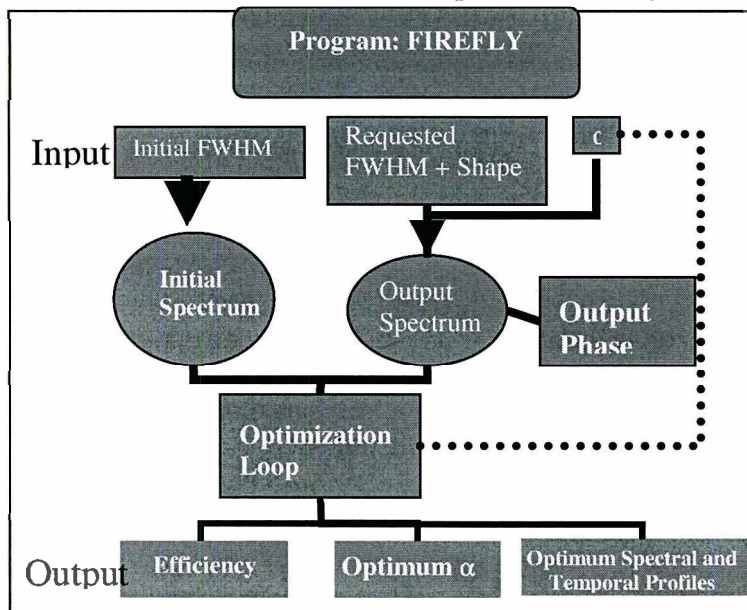


Figure 6: A schematic diagram of the workings of FIREFLY, phase and amplitude modulation program.

we may have to take advantage of the extended spectral wings of the input pulse that are not easily visible in linear graphs such as Fig. 5. We must then force the output spectrum to fall

entirely below the input spectrum (or touching it) everywhere by reducing its spectral amplitude. The consequence of this operation is reduced output energy and reduced throughput efficiency. The name of the process appropriately summarizes this concept: spectral sculpting. Just as a sculptor can never add material to his work, neither can we patch the spectrum. Instead, the desired figure is chipped away from the starting block.

The output spectra for various phase terms (or frequency chirps) are then calculated and fit under the input spectrum from which an optimum output pulse chirp is obtained such that the throughput efficiency reaches a maximum. The more closely the input and output spectra are matched, the greater the throughput efficiency.

FIREFLY furnishes a series of graphs consisting of pulse shapes, spectra, bandwidth, and throughput efficiency as a function of their phase modulation parameters. In addition, phase terms for each of the input, requested output, trial output, and actual output pulses are also provided by FIREFLY. Nested families of comparative pulses and spectra allow for the study of non-optimal alternatives. Figure 6 displays a flow chart of the operation of the program.

There are several potential implementation opportunities for this program. First, an extension to handle pulse trains is trivial. Second, more complex output pulse shapes may be tested easily for efficiency before experimental implementation. Quite generally, most parameters of the input and output pulses are easily modified making for convenient variable manipulation.

To implement these ideas in computer-operable mathematics we first specify numerically the desired output pulse characteristics as a function of time. Making use of the complex electric field notation the slowly varying amplitude of the electric field is multiplied by a slowly varying phase term

$$E = A(t) \cdot e^{i\phi(t)}, \quad (1)$$

where  $\phi$  is defined by our assumed linear frequency chirp as

$$\phi = \alpha \cdot t^2. \quad (2)$$

The high frequency corresponding to the carrier frequency of light (corresponding to the color of the light) has been neglected. For an N'th order Gaussian the slowly varying electric field amplitude is given by

$$E = e^{-\left(\frac{t}{t_0}\right)^N}, \quad (3)$$

where  $t_0$  is related to the FWHM by

$$t_0 = \frac{t_{FWHM}}{2 \cdot \left(\frac{\ln 2}{2}\right)^{\left(\frac{1}{N}\right)}}. \quad (4)$$

For a conventional Gaussian (N=2),  $E = e^{-\left(t/t_0\right)^2}$ . The intensity is proportional to the square of the electric field,

$$I \propto E^2. \quad (5)$$

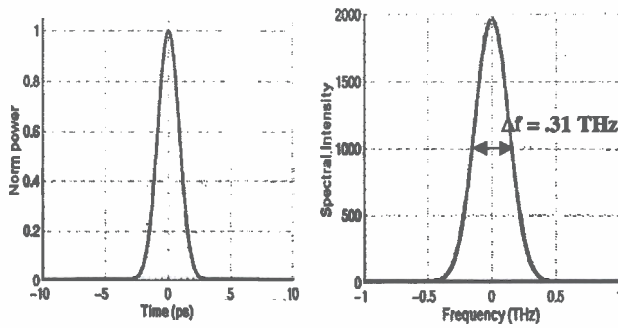


Figure 7: A Gaussian pulse of width 2 ps at FWHM translates to a spectrum of bandwidth 0.31 THz.

In most experiments one measures intensities rather than electric fields, although the field generally contains more detailed information about the phase. The FFT of the field is therefore the useful calculation and reveals the characteristics of the spectrally or temporally varying phase, but the spectral intensity is the useful graph as it represents an easily measured quantity. The square of the magnitude of the

complex Fourier transformed field represents this spectral intensity, just as the square of the electric field in the time domain represents the temporally varying intensity. (Fig.7). Since we have adopted the complex notation of the electric field, the phase angle is given by

$$\phi = \text{Tan}^{-1} \left( \frac{\text{Im}(E)}{\text{Re}(E)} \right)$$

(see Fig. 8), where  $\text{Im}(E)$  and  $\text{Re}(E)$  are the imaginary and the real part of the electric field.

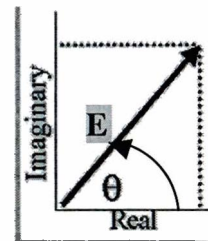


Figure 8: Phase angle is the electric field angle in the complex plane.

**RESULTS AND DISCUSSION:** The results of a series of runs with FIREFLY are very instructive and lead to some generally applicable conclusions.

Figures 9 to 11 contains sample outputs of the program FIREFLY. Figure 9 contains graphs pertaining to one particular Gaussian (N=2) input pulse of 2 ps FWHM and two Gaussian output pulses of 10 ps FWHM. One of the 10 ps Gaussian output pulses is transform-limited while the other one has an imposed optimal frequency chirp for 100% throughput efficiency. Figure 9a displays the short input pulse and the long output pulse once normalized (heavy line) and then properly scaled to the short pulse intensity (dashed line) for the optimum frequency chirp that leads to 100% throughput efficiency (i.e., no energy loss, see Fig. 9c). The transform-limited 10 ps output pulse has a peak intensity approximately 5 times lower than the dashed pulse shown in Fig 9a with a corresponding throughput efficiency of ~ 20%. Figure 9b displays the spectra for the 2 ps input pulse (~0.3 THz bandwidth) and the transform-limited 10 ps output pulse (heavy line). The spectrum for the optimally chirped 10 ps output pulse is identical to that of the input pulse. The spectral phase variations of the output pulses are shown in Fig. 9d for the transform-limited output pulse (horizontal line =constant phase) and the optimally chirped pulse (parabola). The maximum phase excursion over three times the bandwidth (~1 THz) is ~81 radians. Of course, a typical phase filter would not span the 81 rad but rather cover only the range between 0 and  $2\pi$  phase shifts with appropriate multiples of  $2\pi$  subtracted from the phase drawn in Fig. 9d.

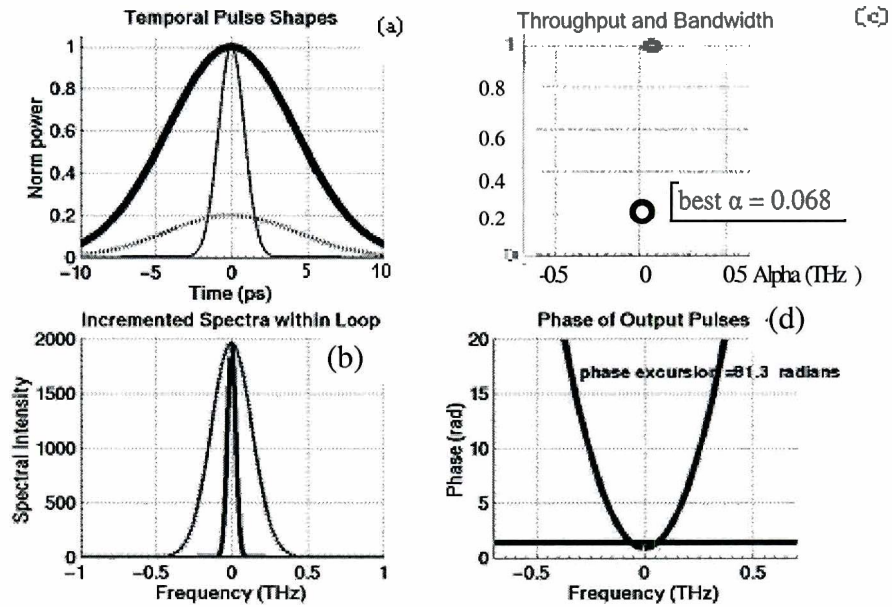


Figure 9: Input (thin), requested output (thick), and actual output (dotted) temporal pulse shapes and spectra, as well as parabolic phase applied to achieve actual output spectrum.

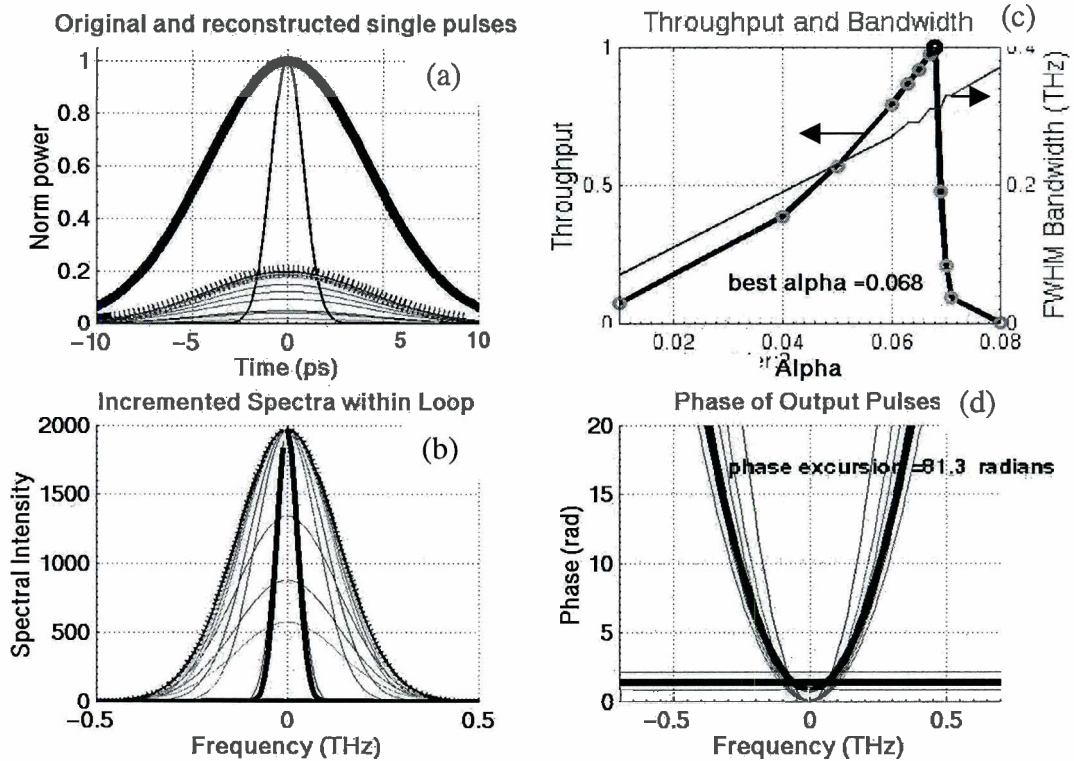


Figure 10: The continuation of the program run from figure 8a shows temporal and frequency domain pulse families, as well as a completed throughput graph for all evaluated  $\alpha$ .

Each of the initial pulse shapes have 10 ps FWHM but the highest peak amplitude is reached for the optimally chirped pulse (same as in Fig. 9), while smaller or larger chirps lead to smaller peak amplitudes and correspondingly smaller throughput efficiencies (Fig. 10a-c). The spectra are seen to gradually broaden (Fig. 10c), until the input spectrum is exceeded, at which point the spectral amplitudes must be reduced to fit under the input spectrum. Note that we have arbitrarily chosen a frequency cut-off point at  $\pm 0.75$  THz beyond which we did not force the output spectrum to lie below the input spectrum. Since there is no appreciable spectral intensity beyond that point this does not introduce a significant error. However, in the strictest interpretation of the spectral shaping philosophy the throughput efficiency would drop to zero for an arbitrarily small incremental increase in bandwidth beyond the optimum. The throughput efficiency (thick line) and bandwidth (thin line) of the output pulses with varying phase parameter  $\alpha$  are shown in Fig. 10b. The throughput gradually increases up to 100% and drops precipitously beyond that while the bandwidth continues to increase monotonically.

From Fig. 10c it is easily seen that beyond the optimum frequency chirp the throughput efficiency drops extremely rapidly and any experimental arrangement would best aim at a bandwidth slightly below the optimum bandwidth in order to avoid potentially devastating losses in throughput efficiency for small increases in bandwidth.

Depending on the laser system to which this pulse shaping scheme is to be applied the optimum chirp from a throughput efficiency point of view may not correspond to that of the laser system. The program FIERFLY allows finding a combined optimum by varying the input pulse shape such that the optimum bandwidth and throughput efficiency are indeed obtained near the optimum for the laser system.

Figure 11 displays the output for a super-Gaussian ( $N=4$ ) output pulse shape. We note that the maximum throughput efficiency (Fig. 11c) is significantly lower than for a standard Gaussian (Fig. 10c), as the shapes dictate certain losses. In general, for output pulse shapes that are different from the input pulse shape the maximum throughput efficiency is less than 100% and depends on the particular input and output pulse characteristics.

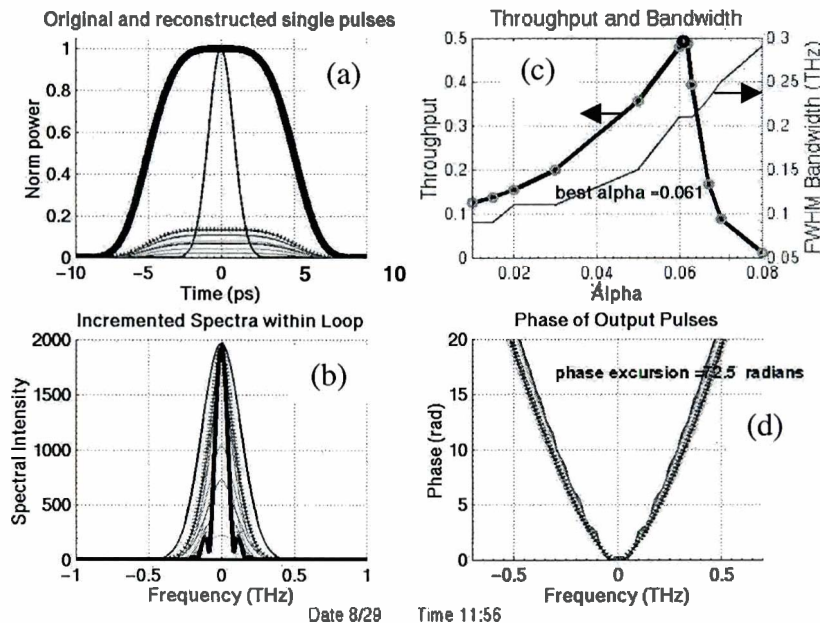
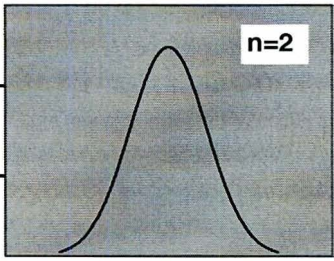
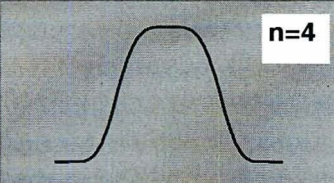


Figure 11: 4<sup>th</sup> order super-Gaussians are able to be created, with lower throughput and larger phase excursions.

Table 1. is a summary of results given by FIREFLY, evidencing the relationship between input, output, and throughput conditions. As shown in Table 1, wider input pulses yield less bandwidth. Since the object is to match the bandwidth of the input pulse, changing that value essentially allows working backwards and optimizing both throughput and bandwidth to optimally fit the laser system.

	Output Pulse Shape	Input FWHM (ps)	Optimum $\alpha$	Throughput	Bandwidth (THz)
Gaussian		1	0.138	100%	0.63
		2	0.068	100%	0.31
		3	0.044	100%	0.21
Super-Gaussian		1	0.183	73%	0.69
		2	0.061	49%	0.21
		1	0.172	69%	0.59

There are several advantages to designing the code using the aforementioned methods and functions. First of all, computer simulations allow for convenient testing, whereas laboratory setups are much more time consuming and expensive. Performing all manipulation in the frequency domain parallels experimental methods, which shape in the fourier plane, i.e., in frequency space. Additionally, arbitrary control of pulse shape and duration is a new and intriguing capability that brings versatility to the shaping process.

The current optimization scheme is based on throughput only but other criteria may be just as important or even more so. Refinements of the present simulations and optimization code could quite easily be implemented and allow for more general optimization schemes as well more general phase modulation schemes beyond the simple linear phase chirp assumed in the present work. Overall, the goals of the present project have been met and the simulation code FIREFLY works quickly and yields useful results.

#### CONCLUSIONS:

Picket pulse shaping through amplitude and phase modulation in the frequency domain has been demonstrated in computer simulations albeit within self-imposed constraints (e.g. linear chirp). In the simulations, transform-limited short laser pulses have been shaped using spectral amplitude and phase control. Gaussian and super-Gaussian pickets have been optimized under hypothetical conditions for energy transfer.

#### REFERENCES:

1. J.E. Rothenberg, "Ultrafast picket fence pulse trains to enhance frequency conversion of shaped inertial confinement fusion laser pulses," Appl. Opt. 39, 6931-6938 (2000).

#### ACKNOWLEDGMENTS:

I would like to send out thanks to the motivators and instigators of my summer's work. Thank you, Dr. Craxton for maintaining this program and allowing us all to be here; Dr. Seka, I'm eternally grateful for your infinite patience and expertise you kindly shared with me; Dr. Zuegel, your perspectives and mantras have been invaluable to me and will not be forgotten; Dr. Marozas, thanks for your explanations and mathematical know-how; Dr. Myatt, for your MATLAB advice. To the rest of the lab, this has truly been an unparalleled experience, and I am grateful to you all for providing this environment.